Numerical stability of 2nd order Runge–Kutta integration algorithms for use in particle–in–cell codes

V. Fuchs

Association EURATOM/IPP.CR,
P. O. Box 17, 18 221 Praha 8, Czech Republic

J. P. Gunn

Association CEA/EURATOM sur la Fusion–Cadarache,
F–13108, France

Received 30 April 2004

An essential ingredient of particle–in–cell (PIC) codes is a numerically accurate and stable integration scheme for the particle equations of motion. Such a scheme is the well known time–centered leapfrog (LF) method [1] accurate to 2nd order with respect to the timestep Δt. However, this scheme can only be used for forces independent of velocity unless a simple enough implicit implementation is possible. The LF scheme is therefore inapplicable in Monte–Carlo treatments of particle collisions [2] and/or interactions with radio–frequency fields [3]. We examine here the suitability of the 2nd order Runge–Kutta (RK) method. We find that the basic RK scheme is numerically unstable, but that conditional stability can be attained by an implementation which preserves phase space area. Examples are presented to illustrate the performance of the RK schemes. We compare analytic and computed electron orbits in a traveling nonlinear wave and also show self–consistent PIC simulations describing plasma flow in the vicinity of a lower hybrid antenna.

PACS: 52.65.Rr, 52.65.Pp
Key words: simulation, tokamak edge plasma, lower hybrid antenna

1 Numerical stability of 2nd order Runge–Kutta integration schemes

In (PIC) simulations with many particles and evolving on long time scales it is essential to use a sufficiently simple, accurate and stable integration scheme for the electron and ion equations of motion

$$dv_{e,i}/dt \equiv \dot{v}_{\mathrm{e,i}} = qE_{\mathrm{z}}/m + a_{\mathrm{e,i}} \quad ; \quad dz/dt \equiv \dot{z} = v\,, \tag{1}$$

where $a_{\mathrm{e,i}}$ are the external acting forces per unit mass, q/m is the particle charge to mass ratio and E_{z} is the self–consistent electric field determined from the Poisson equation. Accuracy and stability of an integration scheme do not go hand–in–hand and need to be discussed separately [4]. Accuracy has to do with the order and magnitude of the lowest order truncation terms, while stability refers to the evolution of numerical perturbations. Here we concentrate on stability. Accuracy is evident from the scheme lowest–order truncation term.

As discussed in detail in [5], E_{z} is only a function of time and particle position. If, in addition, the external forces $a_{\mathrm{e,i}}$ acting on the particles are also independent

of velocity, then the leapfrog method (LF) [1, 4, 5] can be used for integrating the equations of motion (1). In the LF method the particle velocities v and positions z are at each time step Δt advanced as

$$v_{n+1/2} - v_{n-1/2} = \Delta t\, a_n\,, \qquad z_{n+1} - z_n = \Delta t\, v_{n+1/2}\,, \tag{2}$$

where the subscripts indicate time–levels. The LF method is manifestly time–centered and reversible and second order acuracy is easy to verify. Furthermore, the mapping (2) is area–preserving, since its Jacobian is unity:

$$\begin{aligned} J = \det \begin{pmatrix} \partial v_{n+1/2}/\partial v_{n-1/2} & \partial v_{n+1/2}/\partial z_{n-1} \\ \partial z_{n+1}/\partial v_{n-1/2} & \partial z_{n+1}/\partial z_{n-1} \end{pmatrix} \; = \\ = \; \det \begin{pmatrix} 1 & \Delta t\, \partial a_n/\partial z \\ \Delta t & 1 + \Delta t^2 \partial a_n/\partial z \end{pmatrix} \; = \; 1\,. \end{aligned} \tag{3}$$

Area preservation is helpful but does not imply unconditional numerical stability. Instability can arise in difference schemes as a result of normal modes which are not solutions of the exact differential equation. For example, the stability condition for the difference scheme (2) is [4]

$$0 \le -\Gamma \le 2 \quad ; \quad \Gamma = (\partial a/\partial z)\left(\Delta t^2/2\right)\,. \tag{4}$$

For the linear oscillator $a = -\,\omega_0^2\, z$ the condition (4) implies $0 \le \; \omega_0\, \Delta t \; \le 2$. From a purely computational point of view a great advantage of the LF method is that it requires only one evaluation of the force per time step. Unfortunately, LF cannot be used in many situations of physical interest. A significant example of a velocity–dependent force is the Langevin (i.e. Monte Carlo) process [6]

$$\Delta\, v = F\, \Delta t \; + \sigma\, \sqrt{2\, D\, \Delta\, t}\,, \tag{5}$$

which can represent particle velocity–space diffusion due to collisions [2] or radio–frequen-cy heating [3]. In (5) D and F are, respectively, the diffusion and friction coefficients and σ is a normally distributed random variable with zero mean and unity variance.

Our aim is to identify an integration scheme which is not limited to forces independent of velocity and which is numerically not unconditionally unstable. We limit here our attention to the explicit $2^{\rm nd}$ order Runge–Kutta (RK) scheme [7, 8] and suitable modifications thereof. The $2^{\rm nd}$ order RK method [7] for an equation of motion leads to the scheme

$$\begin{aligned} &v_{n+1} - v_n = \tfrac{\Delta t}{2}\left(a_n + a^*_{n+1}\right)\,, \qquad z_{n+1} - z_n = \tfrac{\Delta t}{2}\left(v_n + v^*_{n+1}\right) \\ &v^*_{n+1} = v_n + \Delta t\; a_n\,, \qquad a^*_{n+1} = a_n\left(t_n + \Delta t,\, v_n + \Delta t\, a_n, z_n + \Delta t\, v_n\right)\,, \end{aligned} \tag{6}$$

which requires two evaluations of the applied force, one at $t = t_n$ and one at $t = t_n + \Delta t$. Unlike (2), the scheme (6) is, however, not area preserving since

$$J_{\mathrm{RK}} = 1 + \Delta t \frac{\partial a}{\partial v} + \frac{(\Delta t)^4}{4} \left(\frac{\partial a}{\partial z} \right)^2 \tag{7}$$

A substantial improvement can be immediately obtained by exploiting the property of equations of motion which allow at no extra effort in computation to first evaluate the velocity v_{n+1} and to use that, instead of the anticipated velocity v^*_{n+1}, in the position equation of (6). This modified RK scheme (henceforth denoted by MRK) is therefore partly implicit and its Jacobian is

$$J_{\mathrm{MRK}} = 1 + \Delta t \frac{\partial a}{\partial v} \tag{8}$$

For forces independent of velocity the MRK scheme is therefore area–preserving. The RK schemes are clearly only as good as the approximation (6) for a^*_{n+1}. We will therefore also examine the midpoint Runge–Kutta(MPRK) scheme [8], which likewise requires two evaluations of the force per time–step, one at t and the other at the midpoint $t + \Delta t/2$. The area–preserving form of the MPRK scheme is

$$\begin{array}{l} v_{n+1} - v_n = \Delta t \; a_m \,, \qquad z_{n+1} - z_n = \frac{\Delta t}{2} \, (\, v_n + v_{n+1}) \\ a_m = a_n \, (t_n + \Delta t/2, \; v_n + a_n \Delta t/2, \; z_n + v_n \Delta t/2) \; , \end{array} \tag{9}$$

for which second order accuracy is easy to verify.

We now examine the stability of the RK schemes following the amplification matrix method of Hockney and Eastwood [4]. The present treatment will clarify the role of the Jacobian defined by (3). The above schemes all have the form of a mapping of (v_n, z_n) onto (v_{n+1}, z_{n+1}):

$$v_{n+1} = f(v_n, z_n) \quad ; \quad z_{n+1} = g(v_n, z_n) \tag{10}$$

Perturbations (ϵ_v, ϵ_z) of the variables (v, z) are easily found to satisfy the equation

$$\begin{pmatrix} \varepsilon_v \\ \varepsilon_z \end{pmatrix}_{n+1} = (J) \begin{pmatrix} \varepsilon_v \\ \varepsilon_z \end{pmatrix}_n \quad ; \quad (J) = \begin{pmatrix} \partial f/\partial v_n & \partial f/\partial z_n \\ \partial g/\partial v_n & \partial g/\partial z_n \end{pmatrix} \tag{11}$$

where (J) is the Jacobian matrix. If the eigenvalues λ of (J) lie within or on the unit circle of the complex plane, then perturbations do not grow in the integration process. This is the stability condition. The eigenvalues are obtained from the characteristic equation $\det(J - \lambda) = 0$, i.e. from

$$\lambda^2 - \lambda \, (\partial f/\partial v + \partial g/\partial z) + J = 0 \, . \tag{12}$$

For the LF and the area–preserving RK schemes Eq.(12) becomes

$$\lambda^2 - 2\lambda \, (1 + \Gamma) + 1 = 0 \, , \tag{13}$$

while for the basic RK scheme (6) we obtain

$$\lambda^{\,2} - 2\lambda \, (1 + \Gamma) + 1 + \Gamma^2 = 0 \, . \tag{14}$$

The stability parameter Γ is defined in (4). The roots λ_1 and λ_2 of Eq.(12) satisfy $\lambda_1\lambda_2 = J$. In the interval given by (4) the roots of (13) are complex–conjugate and therefore stable. Elsewhere the area–preserving schemes are unstable. In contrast, the basic RK scheme satisfying (14) is seen to be unconditionally unstable. In the next section 2 we give numerical examples illustrating this.

2 Numerical examples

In order to illustrate the practical performance of the schemes discussed above we now compute electron trajectories in a nonlinear propagating wave, i.e. we solve the equation

$$\dot{v} = \omega\, v_q \cos(\omega\, t - k\, z)\,, \qquad \dot{z} = v\,. \tag{15}$$

Here $v_q = eE_0/m\omega$ is the quiver velocity and E_0 is the applied electric field strength. For our purposes it is important that a first integral of (15) exists in the wave frame of reference. This permits an easy check on the stability of the integration process. With the transformation

$$z' = z - \omega\, t/\, k \quad , \qquad v' = v - \omega\,/\, k \tag{16}$$

the explicit time dependence is removed from (15) and the first integral is

$$v'^2 = {v'_0}^2 + U_0\,(\sin kz' - \sin kz'_0)\,, \tag{17}$$

where $U_0 = 2\omega v_{\rm q}/k$ is the maximum potential energy. When v'^2 is negative in some range of z' then the electron is trapped on a closed orbit within the separatrix. Ideally, the electron will trace the trapped orbit indefinitely, but loss of accuracy and stability of the integration process will lead to departures from the exact orbit. For our example we take $E_0 = 3.5$ kV/cm, $\omega\ = 3.7$ GHz, $k = 750$ m^{-1} and initial conditions $t_0 = 0$, $v_0 = \omega/k$, $k_{z0} = \pi/6$ on a trapped orbit. The reference orbit (17) then has $v'_0 = 0$ and $k'_{z0} = \pi/6$.

We now present some integration results as function of the stability parameter Γ defined in Eq. (4), where ω_0^2 is now replaced by the bounce frequency $\omega_{\rm B}^2 = k\omega v_{\rm q}$. We will compare the exact orbit (17) with LF and RK orbits computed in the fixed reference frame (v, z). The orbits are then transformed to the wave frame via (16).

Figures 1 a,b and 2 compare the exact orbit (17) with the LF and RK orbits. Figure 1a shows the basic RK orbit and Fig. 1b the modified RK orbit for $\Gamma = 0.05$. Even for this small value of the RK orbit has already collapsed and the MRK orbit is starting to spread out. In Figs 2 a,b we show midpoint RK results for $\Gamma = 0.05$, and 0.5, respectively. The MPRK orbits exhibit remarkable stability even as Γ approaches the stability limit. In contrast, the phase space shear of the leapfrog orbits is seen to increase with Γ. This tendency of the leapfrog scheme most likely owes to the phase space shear associated with the shifted velocity and position time levels. This also demonstrates that phase space area preservation does not protect orbits against deformation. An unexpected result, most likely due to a smaller

truncation error, is the superior performance of the MPRK scheme over the MRK scheme.

Next, we present 1–D (toroidal) PIC simulations along a 16 wave–guide lower hybrid (LH) grill [3] surrounded by field–free plasma regions. The boundary conditions are a Maxwellian particle influx to compensate for the outflow. In Eqs (1) the only force acting on the ions is E_Z. In the first case we compute full electron trajectories in the LH grill field $a = v_{\rm q}\cos[\omega t - \varphi(z)]$, where $v_{\rm q}$ is defined after Eq. (15), $\varphi(z)$ is the wave–guide phasing and we integrate Eqs (1) using the leapfrog method. Selected results are shown in Fig. 3. In the second case we represent the electron response by a Langevin process (5), where the diffusion and friction coefficients are given in [3], and we integrate Eqs (1) using the Runge–Kutta method. The results are shown in Fig. 4.

3 Conclusions

We have tested the suitability of $2^{\rm nd}$ order Tunge–Kutta (RK) integration schemes for possible application in PIC codes with the result that schemes presented in the literature [7,8] are numerically unstable with respect to accumulation of round–off errors. However, with an implementation, presented herein, which preserves area in the integration process, stability is achieved under the same conditions as for the leapfrog method. Of the two area–preserving RK methods discussed herein, the midpoint method proves more accurate. We conclude that one extra evaluation of forces is a little price to pay for a Runge–Kutta scheme whose stability is no worse than that of the LF method and which can be easily applied with forces of any type acting on the particles.

References

[1] O. Buneman, J. Comput. Phys. **1** (1967) 517.

[2] W. M. Manheimer, M. Lampe, G. Joyce, J. Comput. Phys. **138** (1997) 563.

[3] V. Fuchs, J. P. Gunn, M. Goniche, V. Petržílka, Nucl. Fusion **43** (2003) 341.

[4] R. W. Hockney, J. W. Eastwood: *Computer Simulation using particles*, Hilger, Bristol, 1988.

[5] C. K. Birdsall, A. B. Langdon: *Plasma Physics via Computer Simulation*, Hilger, Bristol, 1991.

[6] H. Risken: *The Fokker–Planck equation*, Berlin, Springer, 1984, in chapter 3.

[7] M. Abramowitz, I. A. Stegun: *Handbook of Mathematical Functions*, National Bureau of Standards Applied Mathematics Series **55**, Washington D.C., 1964, in chapter 25.

[8] W. H. Press, S. A. Teukolsky, W. T. Vetterling, B. P. Flannery: *Numerical Recipes in Fortran 77*, Cambridge University Press, 1992, in chapter 16.

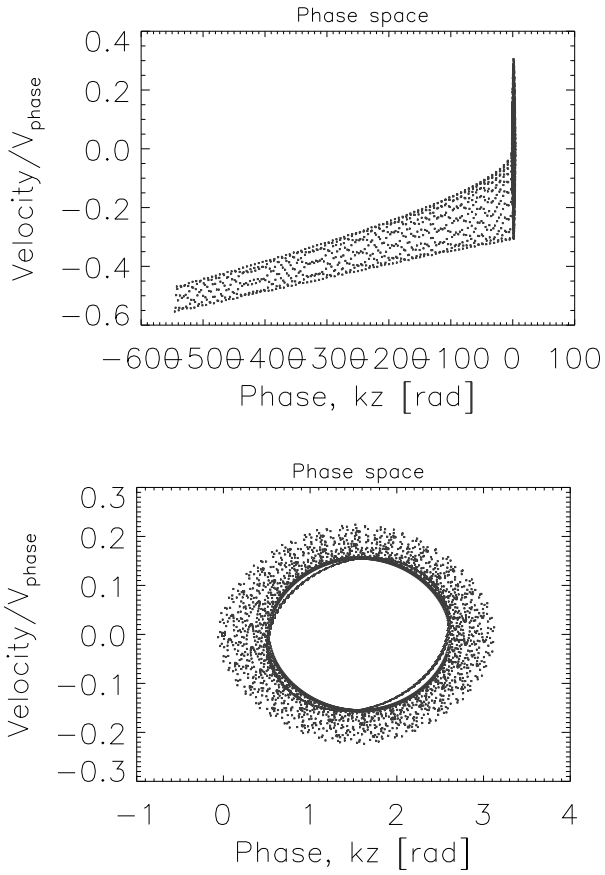

Fig. 1. Exact orbits (17), LF orbits (2), and orbits from a) the basic RK and from b) the MRK schemes (7), for $\Gamma = 0.05$. The basic scheme has collapsed and the MRK orbit is already spreading out.

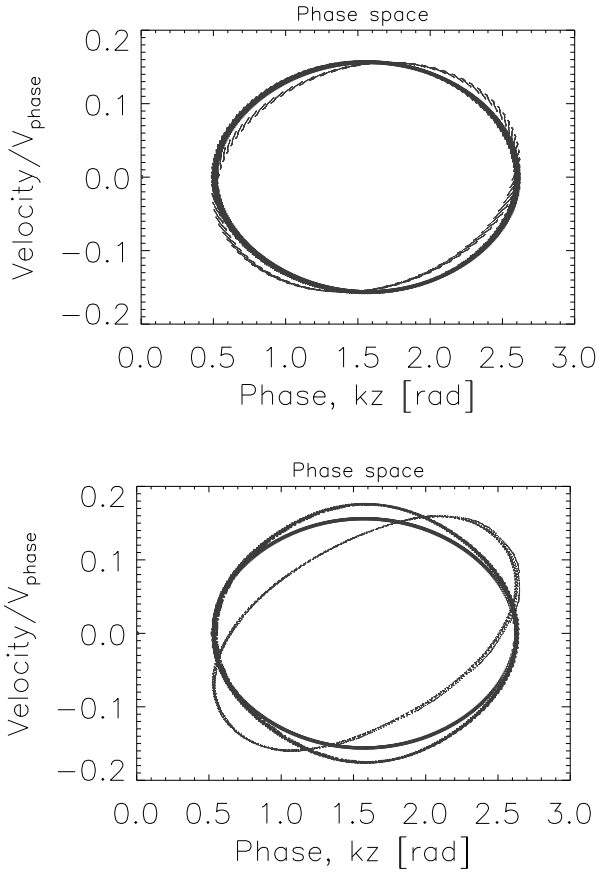

Fig. 2. Exact orbits (17), LF orbits (2), and orbits from the midpoint RK scheme (10) for a) $\Gamma = 0.05$ and b) $\Gamma = 0.5$. In a), the exact and midpoint RK orbits coincide.

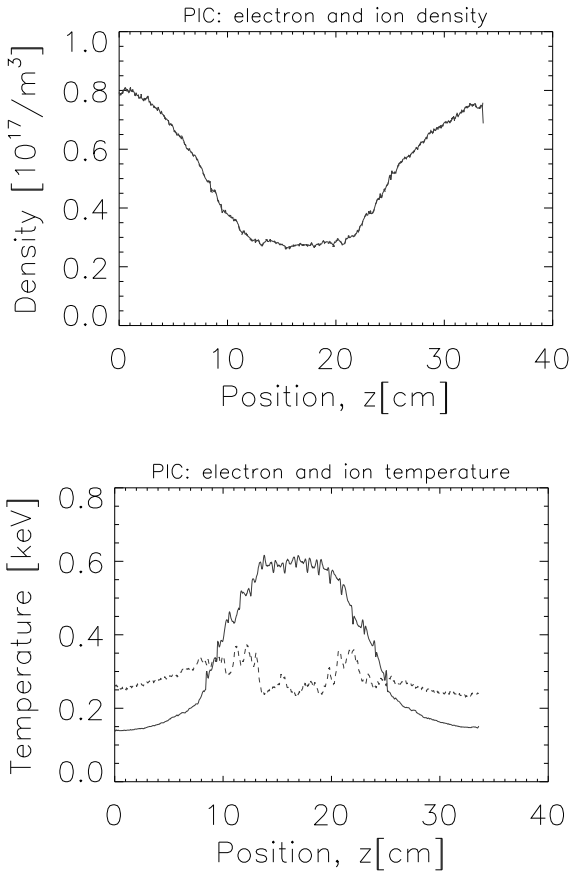

Fig. 3. PIC simulation of plasma response to the LH grill electric field with Newton electron dynamics and the leapfrog integration method. a) The electron and ion densities exhibit a quasi–neutral response. b) Electron and ion temperatures vs position. The electrons, as expected, are strongly heated.

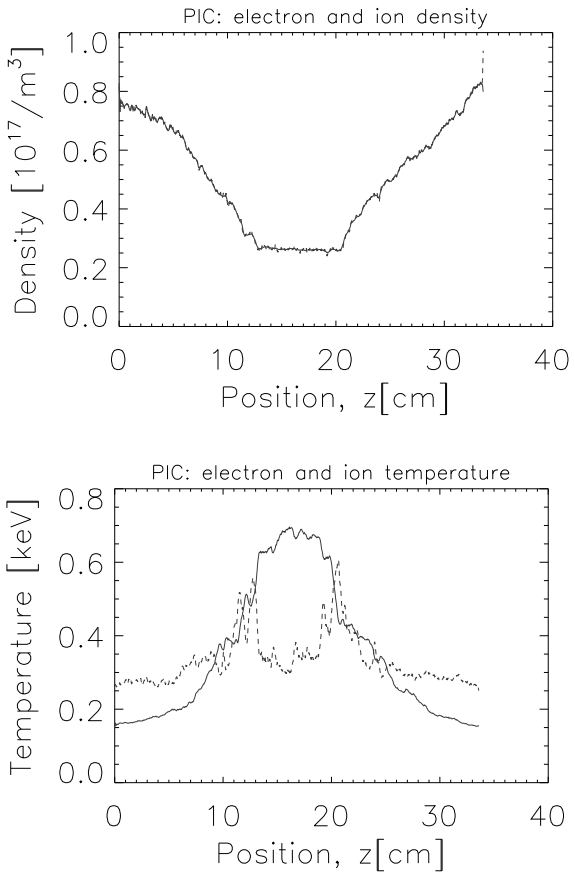

Fig. 4. PIC simulation of plasma response to the LH grill electric field with Langevin electron dynamics and the Runge–Kutta integration method. a) Electron and ion densities and b) electron and ion temperatures vs position.